Molecular dynamics simulations of spin and pure liquids with preservation of all the conservation laws

I. P. Omelyan,[1] I. M. Mryglod,[1,2] and R. Folk[2]
[1]*Institute for Condensed Matter Physics, 1 Svientsitsky Street, UA-79011 Lviv, Ukraine*
[2]*Institute for Theoretical Physics, Linz University, A-4040 Linz, Austria*
(Received 7 December 2000; published 13 June 2001)

A methodology is developed to integrate numerically the equations of motion for classical many-body systems in molecular dynamics simulations. Its distinguishable feature is the possibility to preserve, independently on the size of the time step, all the conservation laws inherent in the description without breaking the time reversibility. As a result, an implicit second-order algorithm is derived and applied to pure liquids, as well as spin liquids, for which the dynamics is characterized by the conservation of total energy, linear and angular momenta, as well as magnetization and individual spin lengths. It is demonstrated on the basis of Lennard-Jones and Heisenberg fluid models that when such quantities as energy and magnetization must be conserved perfectly, the algorithm turns out to be more efficient than popular decomposition integrators and standard predictor-corrector schemes.

DOI: 10.1103/PhysRevE.64.016105 PACS number(s): 02.60.Cb, 75.40.Gb, 75.50.Mm, 76.50.+g

I. INTRODUCTION

During the last years, considerable attention has been focussed on computer studies of relaxation properties and critical phenomena in classical spin systems [1–9]. These studies dealt mainly with lattice models such as the Ising, *XY*, and Heisenberg models. Of current interest is the investigation of continuum spin liquid models [10–15] in which additional dynamical effects are possible because of the coupling between spin and liquid subsystems.

Quite recently [16,17], a set of symplectic algorithms of different orders in the time step has been constructed for numerical integration of motion in the presence of both translational and spin degrees of freedom. As a consequence, the molecular dynamics (MD) simulations of a Heisenberg spin fluid have been carried out. The symplectic integrators were derived by developing the Suzuki-Trotter technique [18] for decompositions of exponential operators. Their main advantages over standard predictor-corrector schemes are explicitness, time reversibility, and exact conservation of spin lengths. It was also shown that the decomposition algorithms permit significantly larger time steps and lead to a substantial speedup of the calculations. In a particular case when the spin degrees of freedom are frozen, these algorithms can be reduced to the well-known velocity Verlet integrator [19], widely used for simulating of pure liquid dynamics.

However, a decomposition (predictor-corrector and other existing traditional numerical schemes [20], such as Runge-Kutta, etc.) approach does not preserve the total energy and magnetization of the system. In most MD applications the accuracy achieved for the energy-magnetization conservation by the decomposition algorithms is high enough to obtain reliable results. Moreover, this accuracy can be improved using higher-order versions [16] of the decomposition approach or decreasing the step size. But if the integrals of motion have to be conserved perfectly, the nonconservative algorithms may not be an optimal choice for the solution of the problem. The reason is that then the time step should be divided into a lot of subintervals, reducing the efficiency of the computations considerably.

The exact conservation of integrals of motion is especially important for simulations of spin liquids near phase transitions, when the phase diagrams, dynamical scaling, long-time correlated behavior, or derivatives of the thermodynamic functions are investigated. This is so because in these cases, the presence of artificial fluctuations in energy and magnetization may have a significant influence on the results. Therefore, it is desirable to look for an algorithm which conserves the fundamental physical invariants exactly or at least within machine accuracy.

In the present paper, a approach to numerical integration of the equations of motion for spin and pure liquids is introduced. The main feature of this approach is its intrinsic preservation of all the conservation laws inherent in the system without violating the time reversibility property. The paper is organized as follows. The basic equations and their integrals of motion are described in Sec. II. Sec III is devoted to a consequent derivation of the desired second-order algorithm. Its possibility to exactly conserve the integrals of motion is demonstrated there also. In Secs. IV and V, the algorithm is tested in actual MD simulations on the Heisenberg and Lennard-Jones fluid models, respectively, and compared with previous numerical schemes. The discussion and concluding remarks are given in Sec. VI.

II. BASIC EQUATIONS OF MOTION AND CONSERVATION LAWS

Let us consider a classical *N*-body system described by the Hamiltonian

$$H=\sum_{i=1}^{N}\frac{m_i\mathbf{v}_i^2}{2}+\frac{1}{2}\sum_{i\neq j}^{N}[\varphi(r_{ij})-J(r_{ij})\mathbf{s}_i\cdot\mathbf{s}_j], \qquad (1)$$

where $\mathbf{r}_i$ and $\mathbf{v}_i$ are the translational position and velocity, respectively, of particle i with mass m_i carrying spin $\mathbf{s}_i$. The fluid part of the potential is denoted by $\varphi(r_{ij})$, whereas

$J(r_{ij})$ is the exchange integral corresponding to a pair of spins with the interparticle separation $r_{ij}=|\mathbf{r}_i-\mathbf{r}_j|$. Note that within the classical approach, each spin $\mathbf{s}_i$ is treated as a continuous three-component vector with fixed length (putting for convenience $|\mathbf{s}_i|=1$, so that J will be measured in energy units). Although the results which will be obtained below can easily be adapted to a larger class of Hamiltonians (to multicomponent systems, for instance), we restrict ourselves for the sake of simplicity to the basic model (1) which represents a typical isotropic Heisenberg spin fluid [12,14]. For $J\equiv 0$, Eq. (1) reduces to a pure liquid model.

In MD simulations it is necessary to solve numerically the equations of motion $d\boldsymbol{\rho}/dt=[\boldsymbol{\rho},H]$, where $[\ ,\ ]$ denotes the Poisson bracket and $\boldsymbol{\rho}\equiv\{\mathbf{r}_i,\mathbf{v}_i,\mathbf{s}_i\}$ is the full set of microscopic phase variables. For the system under consideration, the dynamical equations can be written more explicitly [12,17],

$$\begin{aligned}\frac{d\mathbf{r}_i}{dt}&=\mathbf{v}_i,\\ \frac{d\mathbf{v}_i}{dt}=\frac{\mathbf{f}_i}{m_i}&\equiv-\frac{1}{m_i}\sum_{j(\neq i)}^{N}\left(\frac{\partial\varphi_{ij}}{\partial r_{ij}}-\frac{\partial J_{ij}}{\partial r_{ij}}\mathbf{s}_i\cdot\mathbf{s}_j\right)\frac{\mathbf{r}_{ij}}{r_{ij}},\\ \frac{d\mathbf{s}_i}{dt}&=\frac{\mathbf{s}_i}{\hbar}\times\mathbf{g}_i\equiv\frac{\mathbf{s}_i}{\hbar}\times\sum_{j(\neq i)}^{N}J_{ij}\mathbf{s}_j.\end{aligned}\tag{2}$$

Here, $\mathbf{f}_i=\Sigma_{j(\neq i)}\mathbf{f}_{ij}$ and $\mathbf{g}_i=\Sigma_{j(\neq i)}\mathbf{g}_{ij}$ are the force and internal magnetic field, respectively, acting on particle i due to the interactions $\mathbf{f}_{ij}=-(\varphi'_{ij}-J'_{ij}\,\mathbf{s}_i\cdot\mathbf{s}_j)\mathbf{r}_{ij}/r_{ij}$ and $\mathbf{g}_{ij}=J_{ij}\mathbf{s}_j$ with all the rest of bodies, where $\varphi_{ij}\equiv\varphi(r_{ij})$ and $J_{ij}\equiv J(r_{ij})$. Note that the quantum Poisson bracket was applied [5,12] to derive the equations for spin subdynamics. If an initial state $\boldsymbol{\rho}(0)$ is specified, the time evolution $\boldsymbol{\rho}(t)$ can be uniquely obtained by integrating Eq. (2).

Taking into account the symmetry $\varphi_{ij}=\varphi_{ji}$ and $J_{ij}=J_{ji}$ of interaction potentials, it follows from Eq. (2) that the total energy $E\equiv H$, the total magnetization $\mathbf{M}=\Sigma_i\mathbf{s}_i$, the total linear momentum $\mathbf{P}=\Sigma_i m_i\mathbf{v}_i$, as well as angular momentum $\mathbf{L}=\Sigma_i m_i\mathbf{r}_i\times\mathbf{v}_i$ are integrals of motion, i.e., $dE/dt=d\mathbf{M}/dt=d\mathbf{P}/dt=d\mathbf{L}/dt=0$. The structure of spin equations of motion [the last line of Eq. (2)] imposes in addition the conservation of individual spin lengths $|\mathbf{s}_i|=s_i=\text{const}$. Indeed, $ds_i/dt=d(\mathbf{s}_i\cdot\mathbf{s}_i)^{1/2}/dt=(\mathbf{s}_i\cdot d\mathbf{s}_i/dt)/s_i\equiv\mathbf{s}_i\cdot[\mathbf{s}_i\times\mathbf{g}_i]/\hbar s_i=0$, because the equality $\mathbf{a}[\mathbf{a}\times\mathbf{b}]=0$ is valid for arbitrary vectors $\mathbf{a}$ and $\mathbf{b}$. In addition, the exact solutions are time reversible, since the equations of motion are invariant with respect to the time inversion transformation $t\to-t$, $\{\mathbf{v}_i,\mathbf{s}_i\}\to\{-\mathbf{v}_i,-\mathbf{s}_i\}$.

No existing numerical scheme can obey perfectly all the just mentioned properties. The exact conservation during the integration can be achieved only for some of the integrals of motion, such as linear momentum, for example. Usually, it is required that the deviations of conservative quantities from their original values to be within an acceptable level of precision. This results, however, in limitations on the size of the time steps which actually can be used for MD simulating.

III. THE METHOD OF INTEGRATION

We will show in this section that it is possible to generate time-reversible microscopic trajectories along of which all the integrals of motion are preserved at arbitrary finite time steps. Our derivation of the desired algorithm is started by considering a midpoint scheme of the second order. According to this scheme, the dynamical variables can be propagated as

$$\boldsymbol{\rho}(t+\tau)=\boldsymbol{\rho}(t)+\tau[d\boldsymbol{\rho}/dt]_{t+\tau/2}+O(\tau^3),$$

where τ is the step size and $O(\tau^3)$ denotes the truncation terms. In view of Eq. (2), the explicit expressions for such a propagation read

$$\begin{aligned}\mathbf{r}_i(t+\tau)&=\mathbf{r}_i(t)+\tau\mathbf{v}_i\left(t+\frac{\tau}{2}\right),\\ \mathbf{v}_i(t+\tau)&=\mathbf{v}_i(t)+\tau\,\mathbf{f}_i\left(t+\frac{\tau}{2}\right)/m_i,\\ \mathbf{s}_i(t+\tau)&=\mathbf{s}_i(t)+\tau[\mathbf{s}_i\times\mathbf{g}_i]_{t+\tau/2}/\hbar,\end{aligned}\tag{3}$$

where the midstep values of $\mathbf{v}_i$, $\mathbf{f}_i$, and $\mathbf{s}_i\times\mathbf{g}_i$ should be specified additionally.

The only way to construct mid-point translational velocities maintaining the time reversibility property is

$$\tau\mathbf{v}_i\left(t+\frac{\tau}{2}\right)=\frac{\tau}{2}[\mathbf{v}_i(t)+\mathbf{v}_i(t+\tau)]+O(\tau^3).\tag{4}$$

The terms $O(\tau^3)$ of third and higher orders can be ignored because the corresponding terms of the same orders have been truncated already within the midpoint approach. Equation (4) represents, in fact, an implicit interpolation formula in which past (at time t), and future (at $t+\tau$) values of dynamical quantities enter symmetrically, assuring automatically the reversibility of the solutions.

In the case of translational forces, there are several possibilities to build the midpoint values. The reason is that the interparticle function $\mathbf{f}_{ij}\equiv\mathbf{f}(\mathbf{r}_{ij},\mathbf{s}_i\cdot\mathbf{s}_j)$ depends explicitly on relative position $\mathbf{r}_{ij}$ and orientation $\mathbf{s}_i\cdot\mathbf{s}_j$ which in turn vary with time. Thus, we can apply the midpoint interpolation either to the function $\mathbf{f}_{ij}$ as a whole, or directly to the dynamical variables $\mathbf{r}_{ij}$ and $\mathbf{s}_i\cdot\mathbf{s}_j$. As a result, two different approaches to the force evaluation may be introduced, namely,

$$\mathbf{f}_{ij}\left(t+\frac{\tau}{2}\right)=\frac{1}{2}[\mathbf{f}(\mathbf{r}_{ij}(t),[\mathbf{s}_i\cdot\mathbf{s}_j]_t)+\mathbf{f}(\mathbf{r}_{ij}(t+\tau),[\mathbf{s}_i\cdot\mathbf{s}_j]_{t+\tau})]$$

and

$$\mathbf{f}_{ij}\left(t+\frac{\tau}{2}\right)=\mathbf{f}\left(\mathbf{r}_{ij}\left(t+\frac{\tau}{2}\right),[\mathbf{s}_i\cdot\mathbf{s}_j]_{t+\tau/2}\right).\tag{5}$$

The last approach requires the knowledge of midpoint values for $\mathbf{r}_{ij}$ and $\mathbf{s}_i\cdot\mathbf{s}_j$. The obvious choice for the relative positions is

$$\mathbf{r}_{ij}\left(t+\frac{\tau}{2}\right)=\frac{1}{2}[\mathbf{r}_{ij}(t)+\mathbf{r}_{ij}(t+\tau)]. \tag{6}$$

The interpolation of the scalar product $[\mathbf{s}_i\cdot\mathbf{s}_j]_{t+\tau/2}$ will be described latter. None of the above approaches for evaluating $\mathbf{f}_{ij}(t+\tau/2)$ can lead to a scheme with exact preservation of the total energy. The energy will only be conserved approximately with the precision within which the microscopic solutions are calculated, i.e., $E(t+\tau)=E(t)+O(\tau^3)$.

We will show now that the second approach [Eq. (5)] can be modified in such a way as to compensate the loss of precision in the total energy. The idea lies in the following. Since, according to Eq. (1), the energy difference $E(t+\tau)-E(t)$ is a function of the quantities $\varphi(r_{ij}(t+\tau))$ and $\varphi(r_{ij}(t))$ as well as $J(r_{ij}(t+\tau))$ and $J(r_{ij}(t))$, it is natural to try to evaluate numerically the partial derivatives $\varphi'(r_{ij})=\partial\varphi/\partial r_{ij}$ and $J'(r_{ij})=\partial J/\partial r_{ij}$ [which appear in Eq. (5) at $t+\tau/2$] in terms of the same quantities, rather than to calculate the derivatives analytically. This is possible because for any function $\xi(r_{ij})$ depending only on the interparticle distance r_{ij} we can write the following two expressions:

$$\frac{d\xi(r_{ij})}{dt}=\frac{\partial\xi}{\partial\mathbf{r}_{ij}}\frac{d\mathbf{r}_{ij}}{dt}=\xi'(r_{ij})\frac{\mathbf{r}_{ij}\cdot\mathbf{v}_{ij}}{r_{ij}}$$

and

$$\left.\frac{d\xi(r_{ij})}{dt}\right|_{t+\tau/2}=\frac{\xi(r_{ij}(t+\tau))-\xi(r_{ij}(t))}{\tau}+O(\tau^2),$$

the combinnation of which gives

$$\left.\frac{\xi'(r_{ij})}{r_{ij}}\right|_{t+\tau/2}=\frac{\xi(r_{ij}(t+\tau))-\xi(r_{ij}(t))}{\tau\,\mathbf{r}_{ij}\left(t+\frac{\tau}{2}\right)\cdot\mathbf{v}_{ij}\left(t+\frac{\tau}{2}\right)}+O(\tau^2), \tag{7}$$

where the midpoint values of relative velocity $\mathbf{v}_{ij}=\mathbf{v}_i-\mathbf{v}_j$ are calculated according to Eq. (4) as

$$\mathbf{v}_{ij}\left(t+\frac{\tau}{2}\right)=\frac{1}{2}[\mathbf{v}_{ij}(t)+\mathbf{v}_{ij}(t+\tau)].$$

Then choosing $\xi\equiv\varphi,J$, one finds the expression

$$\begin{aligned}\tau\,\mathbf{f}_i\left(t+\frac{\tau}{2}\right)=-\sum_{j(j\neq i)}\frac{\mathbf{r}_{ij}\left(t+\frac{\tau}{2}\right)}{\mathbf{r}_{ij}\left(t+\frac{\tau}{2}\right)\cdot\mathbf{v}_{ij}\left(t+\frac{\tau}{2}\right)}\{&\varphi(r_{ij}(t+\tau))\\&-\varphi(r_{ij}(t))-[J(r_{ij}(t+\tau))-J(r_{ij}(t))]\\&\times[\mathbf{s}_i\cdot\mathbf{s}_j]_{t+\tau/2}\}\end{aligned} \tag{8}$$

for midstep translational forces, where the $O(\tau^3)$ terms have been neglected.

Performing scalar multiplication of Eq. (8) with the vector $\mathbf{v}_i(t+\tau/2)$, then taking the sum over all the particles ($i=1,2,\ldots,N$), and using the fact that the double sum obtained in the right-hand side is invariant with respect to the replacements $i\leftrightarrow j$, it can be shown that

$$\begin{aligned}\tau\sum_{i=1}^{N}\mathbf{f}_i\left(t+\frac{\tau}{2}\right)\cdot\mathbf{v}_i\left(t+\frac{\tau}{2}\right)=-\frac{1}{2}\sum_{i\neq j}^{N}\{&\varphi(r_{ij}(t+\tau))\\&-\varphi(r_{ij}(t))-[J(r_{ij}(t+\tau))\\&-J(r_{ij}(t))][\mathbf{s}_i\cdot\mathbf{s}_j]_{t+\tau/2}\}.\end{aligned}$$

Assuming for the moment that spin degrees of freedom are frozen (i.e., that $[\mathbf{s}_i\cdot\mathbf{s}_j]$ does not depend on time), the last relation can be presented in the form

$$\tau\sum_{i=1}^{N}\mathbf{f}_i(t+\tau/2)\cdot\mathbf{v}_i(t+\tau/2)=U(t)-U(t+\tau),$$

where U denotes the potential energy of the system. On the other hand, multiplying the second line of Eq. (3) by $\mathbf{v}_i(t+\tau/2)$ and summating over the particles yields

$$\begin{aligned}&\sum_i\frac{m_i}{2}(\mathbf{v}_i(t+\tau)-\mathbf{v}_i(t))\cdot(\mathbf{v}_i(t+\tau)+\mathbf{v}_i(t))\\&\quad\equiv K(t+\tau)-K(t)=\tau\sum_{i=1}^{N}\mathbf{f}_i\left(t+\frac{\tau}{2}\right)\cdot\mathbf{v}_i\left(t+\frac{\tau}{2}\right),\end{aligned}$$

where K denotes the kinetic energy. We see, therefore, that during the time propagation given by Eqs. (3) and (8), the total energy $E=K+U$ is conserved exactly for any τ, i.e., $E(t+\tau)=E(t)$.

Note that Eqs. (7) and (8) are well defined when the scalar product $\mathbf{r}_{ij}(t+\tau/2)\mathbf{v}_{ij}(t+\tau/2)$ tends to zero. This is so because according to the first line of Eq. (3), the midstep relative velocity is connected with the change in position by the constraint $\mathbf{v}_{ij}(t+\tau/2)=(\mathbf{r}_{ij}(t+\tau)-\mathbf{r}_{ij}(t))/\tau$. So that the scalar product is merely equal to $(\mathbf{r}_{ij}(t+\tau)+\mathbf{r}_{ij}(t))\cdot(\mathbf{r}_{ij}(t+\tau)-\mathbf{r}_{ij}(t))/(2\tau)\equiv(r_{ij}(t+\tau)+r_{ij}(t))(r_{ij}(t+\tau)-r_{ij}(t))/(2\tau)$. As a result, the right-hand side of Eq. (7) can be rewritten in the following mathematically equivalent form:

$$\frac{\xi(r_{ij}(t+\tau))-\xi(r_{ij}(t))}{r_{ij}(t+\tau)-r_{ij}(t)}\frac{2}{r_{ij}(t)+r_{ij}(t+\tau)}+O(\tau^2), \tag{9}$$

which reduces to $\xi'(r_{ij}(t+\tau/2))/r_{ij}(t+\tau/2)+\epsilon^2O(\tau^2)$ when the value $|r_{ij}(t+\tau)-r_{ij}(t)|<\epsilon$ is small enough, where $r_{ij}(t+\tau/2)=(r_{ij}(t)+r_{ij}(t+\tau))/2$ and ϵ^2 denotes a machine zero.

The exact energy conservation can also be achieved in the presence of spin subdynamics. In order to show this, unfreeze now the spin variables, and consider first the question of how to interpolate the vector product $\mathbf{s}_i\times\mathbf{g}_i$ arising in the third line of Eq. (3). Again, since this product depends on

time implicitly via dynamical variables $\mathbf{s}_i$ and $\mathbf{g}_i$, we will have here a lot of possibilities. The first of them,

$$[\mathbf{s}_i\times\mathbf{g}_i]_{t+\tau/2}=\frac{1}{2}[\mathbf{s}_i(t)\times\mathbf{g}_i(t)+\mathbf{s}_i(t+\tau)\times\mathbf{g}_i(t+\tau)],$$

is not suitable because it does not lead to the conservation of individual spin lengths, i.e., $s_i(t+\tau)=s_i(t)+O(\tau^3)$. At the same time, the second interpolation

$$[\mathbf{s}_i\times\mathbf{g}_i]_{t+\tau/2}=\frac{1}{2}[\mathbf{s}_i(t)+\mathbf{s}_i(t+\tau)]\times\mathbf{g}_i\left(t+\frac{\tau}{2}\right) \tag{10}$$

does conserve spin lengths exactly, $s_i(t+\tau)=s_i(t)$, for arbitrary choice of $\mathbf{g}_i(t+\tau/2)$. Indeed, substituting Eq. (10) into the propagation equation $\mathbf{s}_i(t+\tau)=\mathbf{s}_i(t)+\tau[\mathbf{s}_i\times\mathbf{g}_i]_{t+\tau/2}/\hbar$ and solving analytically the obtained expression with respect to $\mathbf{s}_i(t+\tau)$, one obtains

$$\begin{aligned}\mathbf{s}_i(t+\tau)=\frac{1}{1+(\tau^2/4\hbar^2)[\mathbf{g}_i]^2_{t+\tau/2}}\Bigg\{&\mathbf{s}_i(t)+\frac{\tau}{\hbar}\mathbf{s}_i(t)\\&\times[\mathbf{g}_i]_{t+\tau/2}+\frac{\tau^2}{4\hbar^2}[2[\mathbf{g}_i]_{t+\tau/2}([\mathbf{g}_i]_{t+\tau/2}\cdot\mathbf{s}_i(t))\\&-([\mathbf{g}_i]_{t+\tau/2})^2\mathbf{s}_i(t)]\Bigg\}.\end{aligned} \tag{11}$$

As can be verified readily, Eq. (11) represents an unitary transformation, $\mathbf{s}_i(t+\tau)=\mathbf{\Theta}_i(t,\tau)\mathbf{s}_i(t)$, where $\mathbf{\Theta}_i(t,\tau)$ is a rotation matrix which, of course, does not change the norm of vectors.

Three different time-reversible interpolations can be introduced for the factor $[\mathbf{g}_i]_{t+\tau/2}\equiv\mathbf{g}_i(t+\tau/2)=\Sigma_{j(j\neq i)}\times[\mathbf{g}_{ij}]_{t+\tau/2}$. They are

$$[\mathbf{g}_{ij}]_{t+\tau/2}=\frac{J(r_{ij}(t))\mathbf{s}_j(t)+J(r_{ij}(t+\tau))\mathbf{s}_j(t+\tau)}{2},$$

$$[\mathbf{g}_{ij}]_{t+\tau/2}=J\left(\frac{r_{ij}(t)+r_{ij}(t+\tau)}{2}\right)\frac{\mathbf{s}_j(t)+\mathbf{s}_j(t+\tau)}{2},$$

and

$$[\mathbf{g}_{ij}]_{t+\tau/2}=\frac{J(r_{ij}(t))+J(r_{ij}(t+\tau))}{2}\,\frac{\mathbf{s}_j(t)+\mathbf{s}_j(t+\tau)}{2}. \tag{12}$$

The first approximation cannot be chosen for our purpose because it destroys the total magnetization of the system, i.e., $\mathbf{M}(t+\tau)=\mathbf{M}(t)+O(\tau^3)$. The last two interpolations do reproduce the magnetization vector perfectly. Indeed, summing up the individual spin propagation [third of Eqs. (3)] over all the particles and taking into account Eq. (10) gives $\mathbf{M}(t+\tau)=\mathbf{M}(t)+\Delta\mathbf{M}$, where

$$\begin{aligned}\Delta\mathbf{M}=\frac{\tau}{4\hbar}\sum_{i\neq j}J_{ij}\left(t+\frac{\tau}{2}\right)&[\mathbf{s}_i(t)+\mathbf{s}_i(t+\tau)]\\&\times[\mathbf{s}_j(t)+\mathbf{s}_j(t+\tau)]\end{aligned}$$

and $J_{ij}(t+\tau/2)$ may be equal either to $J[(r_{ij}(t)+r_{ij}(t+\tau))/2]$ or $[J(r_{ij}(t))+J(r_{ij}(t+\tau))]/2$. The term $\Delta\mathbf{M}$ is canceled because of the invariance of the double sum with respect to the transformation $i\leftrightarrow j$, and of the obvious equality $\mathbf{a}\times\mathbf{b}+\mathbf{b}\times\mathbf{a}=0$ which fulfills for any vectors $\mathbf{a}$ and $\mathbf{b}$. Thus, $\mathbf{M}(t+\tau)=\mathbf{M}(t)$ in both the cases. However, in the first of them when $J_{ij}(t+\tau/2)=J[(r_{ij}(t)+r_{ij}(t+\tau))/2]$, the energy difference $E(t+\tau)-E(t)$, being a function of two quantities $J(r_{ij}(t+\tau))$ and $J(r_{ij}(t))$, cannot be reduced to zero exactly using only one midpoint value $J[(r_{ij}(t)+r_{ij}(t+\tau))/2]$.

At the same time, within the last third interpolation given by Eq. (12) we are able to perform such a reduction. To demonstrate this, let us consider finally the interpolation of the spin scalar product $[\mathbf{s}_i\cdot\mathbf{s}_j]_{t+\tau/2}$ appearing in Eq. (8). Similarly to Eq. (6), one defines this interpolation in the form

$$[\mathbf{s}_i\cdot\mathbf{s}_j]_{t+\tau/2}=\frac{1}{2}[\mathbf{s}_i(t)\cdot\mathbf{s}_j(t)+\mathbf{s}_i(t+\tau)\cdot\mathbf{s}_j(t+\tau)]. \tag{13}$$

Then, using Eqs. (3), (8), (10), and (12), it can be shown that the following equality holds:

$$\begin{aligned}\sum_{i\neq j}^{N}&[J(r_{ij}(t+\tau))-J(r_{ij}(t))][\mathbf{s}_i\cdot\mathbf{s}_j]_{t+\tau/2}\\&=\sum_{i\neq j}^{N}[J(r_{ij}(t+\tau))\mathbf{s}_i(t+\tau)\cdot\mathbf{s}_j(t+\tau)\\&-J(r_{ij}(t))\mathbf{s}_i(t)\cdot\mathbf{s}_j(t)]\equiv U^{(\mathrm{s})}(t)-U^{(\mathrm{s})}(t+\tau),\end{aligned}$$

where $U^{(\mathrm{s})}$ denotes the spin part of the potential energy. So that, as in the case of frozen spin subdynamics, the sum $\tau\Sigma_{i=1}^{N}\mathbf{f}_i(t+\tau/2)\mathbf{v}_i(t+\tau/2)$ is reduced to the potential energy difference $U(t)-U(t+\tau)$. But as was shown earlier using Eq. (3), this sum can be expressed also as the difference $K(t+\tau)-K(t)$ in the kinetic energy. This indicates again that the total energy $E=K+U$ is conserved exactly, i.e., $E(t+\tau)=E(t)$, despite the microscopic solutions $\mathbf{r}_i(t+\tau)$, $\mathbf{v}_i(t+\tau)$, as well as $\mathbf{s}_i(t+\tau)$ are obtained with a limited $O(\tau^3)$ accuracy. It is worth mentioning that the interpolation

$$[\mathbf{s}_i\cdot\mathbf{s}_j]_{t+\tau/2}=\frac{\mathbf{s}_i(t)+\mathbf{s}_i(t+\tau)}{2}\cdot\frac{\mathbf{s}_j(t)+\mathbf{s}_j(t+\tau)}{2}$$

instead of Eq. (13) is possible, in principle, too but it will not lead to the energy conservation.

The approach considered conserves also the total linear and angular momenta, i.e., $\mathbf{P}(t+\tau)=\mathbf{P}(t)$ and $\mathbf{L}(t+\tau)=\mathbf{L}(t)$. The first follows directly from the structure of midpoint translational forces (8) for which $\Sigma_i\mathbf{f}_i(t+\tau/2)=0$, so that

$$\sum_i m_i\mathbf{v}_i(t+\tau)=\sum_i m_i\mathbf{v}_i(t).$$

Further, taking into account Eqs. (3) and (4), the position propagation can be cast as

$$\mathbf{r}_i(t+\tau)=\mathbf{r}_i(t)+\mathbf{v}_i(t)\,\tau+\mathbf{f}_i\left(t+\frac{\tau}{2}\right)\tau^2/2m_i\,.$$

Then the sum $\Sigma_i m_i \mathbf{r}_i(t+\tau)\times\mathbf{v}_i(t+\tau)$ reduces to $\Sigma_i m_i \mathbf{r}_i(t)\times\mathbf{v}_i(t)+\tau\Sigma_i \mathbf{r}_i(t+\tau/2)\times\mathbf{f}_i(t+\tau/2)$. The last term is canceled since, according to Eq. (8), the interparticle forces are parallel to midstep vectors $\mathbf{r}_{ij}(t+\tau/2)$ and, thus, the second property

$$\sum_i m_i\mathbf{r}_i(t+\tau)\times\mathbf{v}_i(t+\tau)=\sum_i m_i\mathbf{r}_i(t)\times\mathbf{v}_i(t)$$

is also satisfied.

Thus, the desired algorithm of the second order has been constructed. In view of Eqs. (3), (4), (6)–(10), (12), and (13), the algorithm can be presented in the following compact form:

$$\mathbf{r}_i(t+\tau)=\mathbf{r}_i(t)+\frac{\tau}{2}[\mathbf{v}_i(t)+\mathbf{v}_i(t+\tau)],$$

$$\mathbf{v}_i(t+\tau)=\mathbf{v}_i(t)-\frac{\tau}{m_i}\sum_{j(\neq i)}\frac{\mathbf{r}_{ij}(t)+\mathbf{r}_{ij}(t+\tau)}{r_{ij}(t)+r_{ij}(t+\tau)}\times\left(\frac{\varphi(r_{ij}(t+\tau))-\varphi(r_{ij}(t))}{r_{ij}(t+\tau)-r_{ij}(t)}-\frac{J(r_{ij}(t+\tau))-J(r_{ij}(t))}{r_{ij}(t+\tau)-r_{ij}(t)}\times\frac{\mathbf{s}_i(t)\cdot\mathbf{s}_j(t)+\mathbf{s}_i(t+\tau)\cdot\mathbf{s}_j(t+\tau)}{2}\right),$$

$$\mathbf{s}_i(t+\tau)=\mathbf{s}_i(t)+\frac{\tau}{\hbar}\frac{\mathbf{s}_i(t)+\mathbf{s}_i(t+\tau)}{2}\times\sum_{j(\neq i)}\frac{J(r_{ij}(t))+J(r_{ij}(t+\tau))}{2}\frac{\mathbf{s}_j(t)+\mathbf{s}_j(t+\tau)}{2}. \tag{14}$$

Equation (14) constitutes, in fact, a coupled system of three nonlinear vector equations for each particle with respect to the same number of unknowns $\mathbf{r}_i(t+\tau)$, $\mathbf{v}_i(t+\tau)$, and $\mathbf{s}_i(t+\tau)$. The system can be solved in a quite efficient way by iteration, letting initially $\mathbf{v}_i^{(0)}(t+\tau)=\mathbf{v}_i(t)$ and $\mathbf{s}_i^{(0)}(t+\tau)=\mathbf{s}_i(t)$ on the right-hand sides of Eq. (14). Then the current values for $\mathbf{r}_i(t+\tau)$, $\mathbf{v}_i(t+\tau)$, and $\mathbf{s}_i(t+\tau)$ obtained on the left-hand sides of Eq. (14) are treated as initial guesses for the next iteration. Already two iterations are sufficient to reach the $O(\tau^3)$ accuracy for the microscopic solutions and energy conservation, i.e., $E(t+\tau)-E(t)=O(\tau^3)$. The goal of carrying out further several updates of Eq. (14) is to reduce the uncertainty $\varepsilon=E(t+\tau)-E(t)$ in energy deviation to a negligibly small value (by adjusting the number $l\geqslant 2$ of iterations for a given τ). The rapid convergence $\varepsilon\rightarrow+0$ is guaranteed by the relative smallness of the step size τ and an exponential decaying of ε with increasing l (see the next section).

It is interesting to remark that the total linear and angular momenta are conserved exactly within each iteration of Eq. (14). The reason is that the interparticle forces are evaluated exploiting Newton's third law and the velocities $\mathbf{v}_i(t+\tau)$ are updated before all $(i=1,2,\ldots,N)$ the advanced positions $\mathbf{r}_i(t+\tau)$ were calculated. For similar reasons, the magnetization conservation is also fulfilled for each iteration, when the spins are updated according to the third line of Eq. (14). In this case, however, the individual spin lengths will only be preserved like energy in an iterative sense, i.e., $\mathbf{s}_i(t+\tau)-\mathbf{s}_i(t)=O(\varepsilon)$. Nevertheless, the spin lengths can be maintained exactly within each iteration by replacing this third line by its mathematically equivalent counterpart (11) [were $[\mathbf{g}_i]_{t+\tau/2}$ is evaluated with the help of Eq. (12)].

IV. NUMERICAL TESTS: COMPARISON WITH OTHER METHODS

In our MD simulations of the Heisenberg spin fluid [Eq. (1)], the Yukawa function [14]

$$Y(r)=w\frac{\sigma}{r}\exp\left(\frac{\sigma-r}{\sigma}\right) \tag{15}$$

was used to describe the spin-spin interactions. The liquid subsystem was modelled by a soft-core potential [21]

$$\varphi(r)=4u\left[\left(\frac{\sigma}{r}\right)^{12}-\left(\frac{\sigma}{r}\right)^{6}\right]+u \tag{16}$$

which accepts nonzero values at $r<2^{1/6}\sigma$ and $\varphi(r)=0$ at $r\geqslant 2^{1/6}\sigma$. Here σ is the diameter of particles, and u as well as w denote the intensities of core-core and spin-spin interactions, respectively. The simulations were carried out in a microcanonical ensemble for $N=1000$ identical $(m_i\equiv m, s_i\equiv 1)$ particles in a cubic box of volume $V=L^3$ employing periodic boundary conditions. The Yukawa function was truncated at $R_c=2.5\sigma<L/2$ and shifted to be zero at the truncation point to avoid the force singularities, i.e., $J(r)=Y(r)-Y(R_c)$ at $r<R_c$ and $J(r)=0$ otherwise. We have chosen the same thermodynamic point as considered in previous papers [16,17], namely, a reduced density of $n^*=N\sigma^3/V=0.6$, a reduced temperature of $T^*=k_BT/w=1.5<T_c^*$ (where k_B is the Boltzmann's constant and $T_c^*\approx 2.055$ the critical temperature of the system [22]), and a nonzero magnetization per particle of $|\mathbf{M}|/N=0.6536$ as well as the same values for the reduced core intensity $u/w=1$ and the dynamical coupling parameter $d=\sigma(mw)^{1/2}/\hbar=2$.

The equations of motion were solved using a well established Adams-Bashforth-Moulton (ABM) predictor-corrector integrator of the fourth order [20], the explicit decomposition schemes [16,17] of the second (ED) and forth (ED4) orders, as well as our conservative spin fluid dynamics (CSFD) algorithm [Eq. (14)]. All the test runs were started from an identical well equilibrated configuration. A typical example

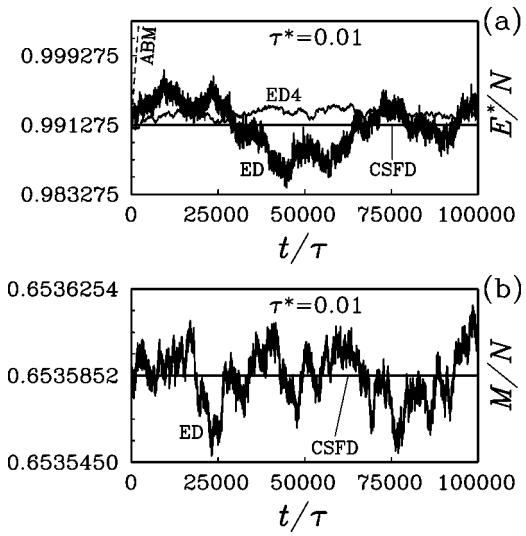

FIG. 1. The total energy E^*/N (a) and magnetization M/N (b) per particle as functions of the length t/τ of the simulations performed for a Heisenberg spin fluid using the predictor-corrector [dashed curve in (a), marked ABM], decomposition (solid curves, ED/ED4), and our algorithms (bold solid horizontal lines, CSFD). Note that the ABM and ED4 curves are indistinguishable in (b) from the CSFD line.

for the reduced total energy $E^*=E/w$ and magnetization $M=|\mathbf{M}|$ per particle as depending on the length of the simulation is shown in subsets (a) and (b) of Fig. 1, respectively, at a reduced time step of $\tau^*=\tau(w/m\sigma^2)^{1/2}=0.01$.

The huge systematic deviations in the total energy obtained within the ABM approach [see the dashed curve in Fig. 1(a)] points out clearly that it is highly unstable and, thus, not suitable for long-duration observations over the system at the time step considered. We mention that in the ABM scheme, the dynamical variables are first predicted,

$$\boldsymbol{\rho}(t+\tau)=\boldsymbol{\rho}(t)+[55\dot{\boldsymbol{\rho}}(t)-59\dot{\boldsymbol{\rho}}(t-\tau)+37\dot{\boldsymbol{\rho}}(t-2\tau)$$

$$-9\dot{\boldsymbol{\rho}}(t-3\tau)]\frac{\tau}{24}+O(\tau^5),$$

and further iteratively corrected as

$$\boldsymbol{\rho}(t+\tau)=\boldsymbol{\rho}(t)+[9\dot{\boldsymbol{\rho}}(t+\tau)+19\dot{\boldsymbol{\rho}}(t)-5\dot{\boldsymbol{\rho}}(t-\tau)$$

$$+\dot{\boldsymbol{\rho}}(t-2\tau)]\frac{\tau}{24}+O(\tau^5),$$

where $\dot{\boldsymbol{\rho}}=\{\mathbf{v}_i,\mathbf{f}_i/m,[\mathbf{s}_i\times\mathbf{g}_i]/\hbar\}$. The strong instability of the ABM integrator can be explained by the facts that it destroys the unit norm of spin lengths (although conserves the magnetization vector) and generates time irreversible solutions (as has been rigorously prover [23], the numerical stability follows directly from the reversibility of an algorithm). For this reason, the ABM as well as other existing predictor-corrector schemes can be used only at very small time steps (namely, at $\tau^*\leqslant 0.00125$, see Refs. [16,17]), where they exhibit similar equivalence in the energy conservation as that of the decomposition algorithms. However, such small step sizes are inefficient, because then too much expensive force and field recalculations have to be performed in order to cover the fixed observation time. Moreover, the ABM scheme is about twice times slower compared to the ED integrator even if one iteration only is applied within the corrector procedure.

No drift in the functions $E(t)$ and $M(t)$ was recognized within both the decomposition ED and ED4 algorithms at time steps up to $\tau^*\equiv\tau^*_{\max}=0.01$ and over a number of time steps of $t/\tau=100\,000$. These algorithms, however, do not conserve the total energy and magnetization exactly. Instead, the last functions fluctuate quite visibly especially in the ED case, as can be seen from Fig. 1. The ED4 energy fluctuations are approximately a factor of 2 smaller than those of the ED algorithm. This compensates the additional processor time needed to evaluate high-order expressions to some extent. However, the ED4 algorithm allows one to reduce the magnetization deviations to a negligibly small level which does not exceed about $\langle[\mathbf{M}(t)-\mathbf{M}(0)]^2\rangle^{1/2}/N\sim 3\times 10^{-9}$ even at the greatest time step $\tau^*_{\max}$, where $\langle\,\rangle$ denotes the microcanonical averaging. It is worth mentioning that the ED/ED4 energy-magnetization fluctuations are caused by the $O(\tau^3)/O(\tau^5)$ truncation errors and thus they will increase drastically with increasing τ.

The situation is completely different in the case of our approach, because the CSFD algorithm preserves the integrals of motion for arbitrary time steps. Of course, we cannot apply too large step sizes ($\tau^*\sim 1$) since then the microscopic solutions will deviate considerably from their exact counterparts and because of too large number of iterations needed to achieve the convergence. Choosing, for instance, $\tau^*\equiv\tau^*_{\max}=0.01$ we have determined the following levels $\mathcal{E}$ in the averaged total energy fluctuations $\mathcal{E}=\langle(E^*(t)-E^*(0))^2\rangle^{1/2}/N$ at the end of the 100 000 time step runs: 9.2×10^{-4}, 2.3×10^{-5}, 3.1×10^{-6}, 2.2×10^{-7}, and 2.8×10^{-8} corresponding to the numbers l of iterations 2, 3, 4, 6, and 8, respectively. We see, therefore, that the iterations converge rapidly with increasing l and the uncertainties can be approximately described by the exponential dependence $\mathcal{E}\sim 3\times 10^{-4}\exp(-1.2l)$ at $l\geqslant 4$. Of course, the iterative solutions require additional computational efforts, but they are justified when a high level of the energy conservation is necessary. In order to demonstrate this, we have tried to reduce the energy fluctuations within the ED/ED4 algorithms by decreasing the time step. The corresponding result for $\mathcal{E}$ at the time steps 0.01, 0.005, 0.0025, and 0.00125, i.e., at $\tau^*\equiv\tau^*_{\max}/l$ with $l=1$, 2, 4, and 8 is presented in Fig. 2 in comparison with the above CSFD data.

As one can see, such a reduction of the ED/ED4 energy fluctuations is not efficient, since the deviations $\mathcal{E}$ behave as $\sim l^{-2}$, i.e., decrease with increasing l much more slower than the exponential dependence obtained within the CSFD algorithm. In view of the results of Fig. 2 and taking into account that at the same value of l one needs approximately the same processor time with both the ED and CSFD algorithms (the ED4 integrator needs the time larger by factor 5 and is less economical) in order to investigate the system over an identical time interval, we come to the following conclusion:

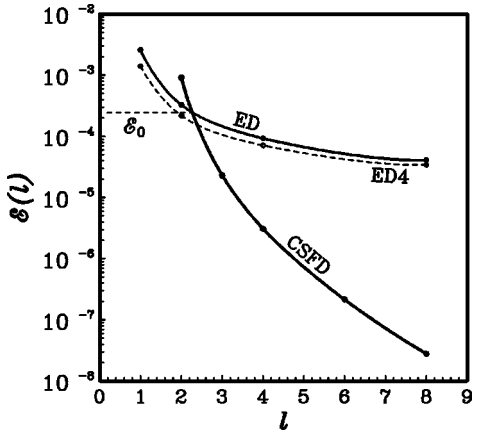

FIG. 2. The averaged total energy fluctuations $\mathcal{E}$ as a function of the number l of iterations, obtained in the Heisenberg fluid simulations within the CSFD algorithm at the reduced time step $\tau^*_{\max}=0.01$ (bold solid curve). The levels of $\mathcal{E}$ corresponding to the decomposition integrators at the time steps $\tau^* \equiv \tau^*_{\max}/l$ are connected by solid (ED) and dashed (ED4) curves.

When the total energy must be conserved up to a precision of $\mathcal{E}_0 \sim 10^{-4}$ (the intersection point of the ED and CSFD curves, see the horizontal dashed line in Fig. 2) or better, the preference should be done to the CSFD algorithm. For example, a level of $\mathcal{E} \sim 10^{-6}$ in the conservation is achieved at $l \sim 5$ within the CSFD algorithm, while up at $l \sim 50$ for the ED scheme (the last value was obtained by extrapolating the $\sim l^{-2}$ dependence to larger l). Thus the CSFD algorithm appears to be approximately in 10 times faster than the ED integrator at this level of $\mathcal{E}$. For $\mathcal{E} > \mathcal{E}_0$, we can restrict ourselves to the usual explicit decomposition integrators.

Note that despite the uncertainties $\mathcal{E}_0 \sim 10^{-4}$ look quite small, they can considerably influence some observable macroscopic quantities. The influence can be estimated quantitatively in terms of the ratio $\Gamma = [\langle (E(t)-E(0))^2 \rangle / \langle (U(t)-U(0))^2 \rangle]^{1/2}$ of total and potential energy fluctuations. For our system $\mathcal{U} = \langle (U^*(t)-U^*(0))^2 \rangle^{1/2}/N \sim 10^{-2}$, where $U^* = U/w$, so that $\Gamma_0 = \mathcal{E}_0/\mathcal{U} \sim 1\%$. Usual investigated quantities, such as thermodynamic functions, structure factors, etc., will be calculated approximately with the same relative precision Γ_0 (provided the averaging over the produced trajectories is performed during a sufficiently large time interval to be entitled to ignore the statistical noise). However, when long-tail time correlation functions or derivatives of the thermodynamic functions are involved in the computations, the impact of the artificial energy fluctuations on the results will be much greater. For instance, the relative uncertainty in the measurements of the specific heat (which are based on a microcanonical ensemble fluctuation formula) is estimated to already be $(\Gamma_0)^{1/2} \sim 10\%$. This uncertainty may appear to be too large to determine correctly a phase diagram of the system.

A similar pattern to that shown in Fig. 2 was observed within the CSFD approach at greater time steps $\tau > 0.01$. The energy as well as magnetization fluctuations continued to damp exponentially with increasing l, although a greater number of the iterations was necessary to reach the same level of the conservation. Note that a rotational matrix version of the CSFD algorithm [when the third line of Eq. (14) is replaced by Eq. (11)], in which individual spin lengths are maintained exactly within each iteration, leads to a somewhat better energy preservation at a given l (but then the total magnetization, similar to the energy, will be conserved in the iterative sense, i.e., at sufficiently large l). The CSFD results presented above for $\mathcal{E}$ have been obtained using this version for spin subdynamics propagations.

Further improvements in the efficiency of the CSFD algorithm can be reached applying the following computational trick. It can occur that after a some period of time during the integration process the energy difference $E(t)-E(0)$ corresponding to the last lth iteration (within a current time step t/τ) exceeds the difference obtained for the previous $(l-1)$-th iteration. Such a situation is possible because of round-off errors and an accumulation of other numerical uncertainties, especially at relatively small values of l, where the lack in the time reversibility can lead to an instability of the solutions (note the CSFD algorithm is time reversible in the iterative sense, i.e., at large enough values of l). Then to avoid the accumulation, we should merely take the values for microscopic phase variables corresponding to this previous $(l-1)$-th iteration. The trick with a flexible number of the iterations will guarantee a good stability for small $l \sim 2-4$ as well.

Another technical detail concerns the way in which the expression $[\xi(r(t+\tau))-\xi(r(t))]/[r(t+\tau)-r(t)]$ [appearing in Eq. (14) for $\xi \equiv \varphi, J$] should be treated in the limit $r(t+\tau) \to r(t)$. As was pointed out earlier, this expression must be computed using its limiting representation $\xi'([r(t)+r(t+\tau)]/2)+\epsilon^2 O(\tau^2)$ when the difference $|r(t+\tau)-r(t)| < \epsilon$ is small enough. Then letting ϵ^2 being equal a machine zero, the truncated term $\epsilon^2 O(\tau^2)$ can be ignored completely. In our program code we have used a double precision throughout with 16 significant digits, $\epsilon^2 = 10^{-16}$, so that the value ϵ was set to be equal to 10^{-8}. It is interesting to remark that the condition $|r_{ij}(t+\tau)-r_{ij}(t)| < \epsilon$ was never achieved for any pair ij of particles during the simulations and, thus, the limiting expression was never used. This can be explained by the fact that the probability of finding the system in such a state is prohibitively small and is proportional to $C\epsilon$. The coefficient C increases with increasing the length of the simulations and the number of particles as $C \sim tN^2$. Thus, the limiting expression is expected to be applied for systems with a greater size or when extra long simulations are performed.

Finally, some words about the angular momentum conservation. As is well known, the periodic boundary conditions, which are commonly used in MD simulations to reduce the finite-size effects, destroy the angular momentum vector. Nevertheless, it has been established that this vector is conserved in our simulations in mean, namely, $\langle \mathbf{L}(t) \rangle \approx \mathbf{L}(0)$. Note that initial values for the total angular as well linear momenta were putted to be equal to zero, $\mathbf{L}(0)=0$ and $\mathbf{P}(0)=0$, i.e., the system was considered at the very beginning as one which does not move as a whole translationally and rotationally.

V. APPLICATIONS TO OTHER SYSTEMS: PURE LIQUIDS AND HARMONIC OSCILLATOR

The algorithm derived in the preceding section can also be applied with equal successes to dynamics simulations of other liquid models. For instance, letting formally $J\equiv 0$, we come to the usual equations of motion corresponding to a pure liquid system. These equations can be integrated using the first two lines of the same propagation equation (14), where the terms with J in the right-hand side of the second line must be omitted (the third line describes spin subdynamics and is not relevant in this case).

Our simulations of pure liquid dynamics were based on a system composed of $N=256$ particles interacting through a cut-off Lennard-Jones (LJ) potential $\varphi(r)=\Phi(r)-\Phi(R_c)$ at $r<R_c=3.25\sigma$ with $\varphi(r)=0$ otherwise, where

$$\Phi=4u\left[\left(\frac{\sigma}{r}\right)^{12}-\left(\frac{\sigma}{r}\right)^{6}\right]. \tag{17}$$

The MD test runs have been performed at a reduced density of $n^*=0.845$ and a reduced temperature of $T^*=k_BT/u=1.7$. For the purpose of comparison, the equations of motion were integrated applying also a well-established velocity Verlet (VV) algorithm [19,23] of the second order and its forth-order (VV4) counterpart [18]. Our algorithm we will now call conservative of pure fluid dynamics (CPFD) algorithm. A typical maximal value for the reduced time step in simulating such a system is $\tau^*_{\max}=\tau(u/m\sigma^2)^{1/2}=0.005$ [24]. All the runs started from a well equilibrated configuration and covered an identical time interval of $t^*=t(u/m\sigma^2)^{1/2}=50$ (corresponding to 10 000 time steps at $\tau^*=0.005$).

It is worth mentioning that the explicit VV integrator propagates the phase variables according to the relations

$$\mathbf{r}_i(t+\tau)=\mathbf{r}_i(t)+\mathbf{v}_i(t)\tau+\mathbf{f}_i(t)\frac{\tau^2}{2m}+O(\tau^3),$$

$$\mathbf{v}_i(t+\tau)=\mathbf{v}_i(t)+[\mathbf{f}_i(t)+\mathbf{f}_i(t+\tau)]\frac{\tau}{2m}+O(\tau^3).$$

This propagation can be presented as

$$\{\mathbf{r}_i(t+\tau),\mathbf{v}_i(t+\tau)\}=\mathbf{D}(t,\tau)\{\mathbf{r}_i(t),\mathbf{v}_i(t)\}+O(\tau^3),$$

where $\mathbf{D}(t,\tau)$ denotes the evolutionary operator. The VV4 algorithm deals (similarly to the ED4 scheme) with the five stages propagation

$$\{\mathbf{r}_i(t+\tau),\mathbf{v}_i(t+\tau)\}=\prod_{k=1}^{5}\mathbf{D}(t,\xi_k\tau)\{\mathbf{r}_i(t),\mathbf{v}_i(t)\}+O(\tau^5),$$

where the coefficients ξ_k are $\xi_1=\xi_2=\xi_4=\xi_5\equiv\xi=1/(4-4^{1/3})$ and $\xi_3=1-4\xi$. The VV approach needs only in one force evaluation (the most time-consuming part of the calculations) per time step, $p_{\rm VV}=1$, while $p_{\rm VV4}=5$. The CPFD algorithm requires two force evaluation per iteration within the time step, i.e., $p_{\rm CPFD}=2$.

The averaged total energy fluctuations $\mathcal{E}=\langle(E(t)-E(0))^2\rangle^{1/2}/(uN)$ obtained within the CPFD integration at the time step $\tau^*_{\max}=0.005$ and the numbers of iterations of $l=2$, 3, 4, and 8 are plotted in Fig. 3 as a function of the reduced processor time lp (where in this case $p=p_{\rm CPFD}$) needed to perform the run of the mentioned above length $t^*=50$. The fluctuations identified during the integration at the time steps $\tau^*=\tau^*_{\max}/l$ using the VV algorithm with $l=1$, 2, 4, 8, and 16 as well as the VV4 algorithm with $l=0.5$, 1, 2, 4 are also included in this figure. The processor time spent to carry out the VV run of the length $t^*=50$ at $\tau^*=0.005$ is assumed to be equal to unity in our dimensionless presentation lp (where $p=1$,2 and 5 for the VV, CPFD, and VV4 integrators).

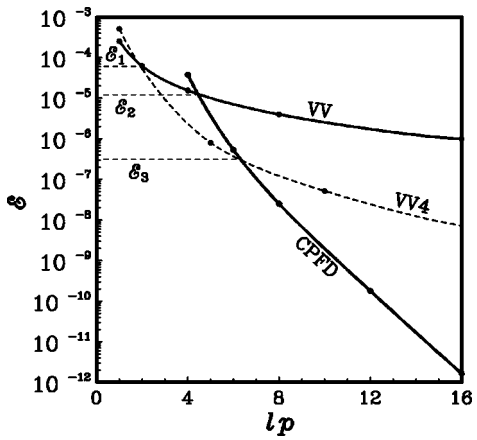

FIG. 3. The averaged total energy fluctuations $\mathcal{E}$ as a function of the reduced processor time lp needed for the simulations of a Lennard-Jones liquid within the CPFD (bold solid curve), usual velocity Verlet (solid curve, VV), and fourth-order velocity Verlet (dashed curve, VV4) algorithms.

The LJ energy fluctuations damp with increasing l as $\sim l^{-2}$, $\sim l^{-4}$, and $\sim\exp(-2.4l)$ within the VV, VV4, and CPFD integrations, respectively. Up to three intersection points corresponding to the VV-VV4, VV4-CPFD, and VV4-CPFD curves with the energy conservation levels of $\mathcal{E}_1\sim 6\times 10^{-5}$, $\mathcal{E}_2\sim 10^{-5}$, and $\mathcal{E}_3\sim 3\times 10^{-7}$ can be observed in Fig. 3. So that the usual VV algorithm is recommended to be used when the precision $\mathcal{E}$ of energy conservation plays not so important role in the computations, namely, when $\mathcal{E}\geqslant\mathcal{E}_1$. The calculation with the help of the VV4 integrator appears to be most computationally efficient in the intermediate regime $\mathcal{E}_3<\mathcal{E}<\mathcal{E}_1$. Finally, when a very accurate conservation $\mathcal{E}<\mathcal{E}_3$, is required, the best choice is to apply the CPFD algorithm because then it becomes to be most economical.

The CPFD approach can also be used for the prediction of dynamical phenomena in other many-body collections (such as the solar system, for instance) and treated as an efficient numerical solver of first-order differential equations. The most notorious example (which can be analyzed analytically) is the equation $d^2x/dt^2\equiv\ddot{x}=-x$ describing dynamics of a simple harmonic oscillator. This equation reduces to a system of two first-order differential equations $\dot{x}=v$ and $\dot{v}=-x$, which in turn can be reproduced from the first two lines of general equation (2) putting formally $\mathbf{r}_i\equiv x$, $\mathbf{v}_i\equiv v$, $\varphi=x^2/2$, $m_i\equiv 1$, and $J=0$. Then in view of Eq. (14), the time

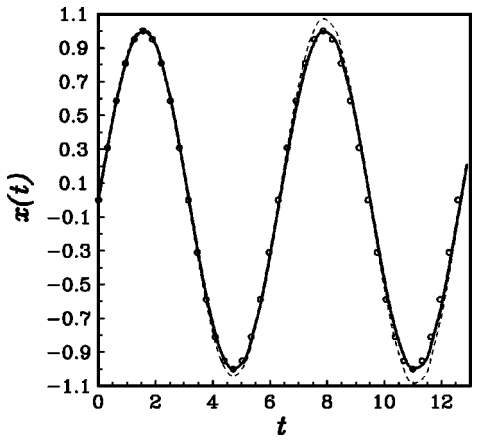

FIG. 4. Numerical solutions to the differential equation $\ddot{x}(t) = -x$ obtained during our new (solid curve) and velocity-Verlet (dashed curve) integrations at the time step $\tau = 0.05T$ with $T = 4\pi$. The exact result $x(t) = \sin(x)$ is shown as open circles.

propagation reads $x(t+\tau) = x(t) + \tau[v(t) + v(t+\tau)]/2$ and $v(t+\tau) = v(t) - \tau[x(t) + x(t+\tau)]$. The last two relations can be solved explicitly, and the result for the conservative numerical trajectories is

$$x(t+\tau) = \frac{x(t)(1-\tau^2/4) + v(t)\tau}{1+\tau^2/4},$$

$$v(t+\tau) = v(t) - \tau\frac{x(t) + v(t)\tau/2}{1+\tau^2/4},$$

whereas the VV solutions are

$$x(t+\tau) = x(t)(1-\tau^2/2) + v(t)\tau,$$

$$v(t+\tau) = v(t) - \tau[x(t)(1-\tau^2/4) + v(t)\tau/2].$$

Choosing the initial conditions $x(0) = 0$ and $\dot{x}(0) \equiv v(0) = 1$, the above two types of numerical trajectories can be compared between themselves and with respect to the exact solution $x(t) = \sin(t)$ and $\dot{x}(t) \equiv v(t) = \cos(t)$. The result of comparison for $x(t)$ is presented in Fig. 4 at a typical time step of $\tau = 0.05T$, where $T = 2\pi$ denotes the period of the oscillations. As can be seen easily, the conservative solution leads to a better reproduction of the original dependence than the VV trajectory, despite the both CPFD and VV approaches are valid to the same $O(\tau^3)$ order in truncation errors. Therefore, additional cancellations of the truncation uncertainties are possible due to the exact preservation of the integral of motion $2E = \dot{x}^2 + x^2 \equiv 1$ along the CPFD trajectory (note that maximal VV deviations in E consist of about 20% at $\tau = 0.05T$). Similar cancellations of the truncation uncertainties in microscopic solutions within our conservative approach should be expected for other systems of differential equations, in particular, for spin and pure liquid dynamics.

VI. CONCLUDING REMARKS

One of the most fundamental characteristics in physics are the conservation laws. Therefore, it is desirable that the numerical methods in computational physics obey these laws. Unfortunately, the most popular algorithms, such as predictor corrector, Runge-Kutta, Verlet, decomposition Suzuki-Trotter, etc., being applied to the nonlinear many-body problem, do not preserve fundamental physical invariants, such as energy and angular momentum, when these are inherent in the description.

In the present paper we have tried to remedy such a situation and formulated a completely conservative approach for numerical integration of the equations of motion in classical systems. The approach is general enough to be used for a wide class of systems such as spin and pure liquids, collections of charged particles, etc. It can also be considered for the prediction of other phenomena in physics, astrophysics, chemistry, and biology, whenever the numerical solutions to systems of differential equations are necessary.

Our main attention in this study was concentrated on dynamics of spin liquid models in which additional effects with respect to pure liquids are possible because of the energy exchange between spin and liquid subsystems [15–17]. As a result, a new second-order MD algorithm (called as CSFD) has been consequently derived within the above presented approach. Its greatest advantage is that all the integrals of motion existing in the system, namely, the total energy, linear and angular momenta, individual spin lengths, and total magnetization are conserved independently on the size of the time step. It is worth emphasizing that such a complete conservation has been achieved intrinsically, i.e., without the introduction of any artificial external forces or numerical constraints. Moreover, the resulting algorithm maintains the time reversibility property inherent in the basic equations. This is also important for long-duration MD observations because the stability of an algorithm is closely connected with its time reversibility [23].

The presented algorithm is implicit, i.e., it requires iterative solutions. Thus, when a high precision in conservation is not needed, the CSFD scheme may be less efficient in practice than explicit decomposition methods [16,17]. We have shown, however, on the basis of an actual simulation of a Heisenberg fluid model that when the total energy and magnetization must be reproduced precisely, the CSFD algorithm may be in order or even more faster than the decomposition integrators. Another important feature of the conservative method is that additional cancellations of the truncation uncertainties are possible in microscopic solutions due to the exact preservation of the macroscopically observable integrals of motion, as was demonstrated analytically on a simple example of the harmonic oscillator.

For a particular case when the spin subsystem is absent, the CSFD algorithm reduces to a so-called CPFD integrator. While this work has been done we have learned that this integrator is equivalent, in fact, to that developed independently by Greenspan [25] as well as Gonzalez and Simo [26]. These authors, however, considered the integration in respect of applying it to mechanical systems when the number of particles is not very large. Here we have shown within the LJ model that the CPFD integrator can be used with equal success in MD simulations of pure liquids.

The approach presented can be adapted to many-component systems, optimized to a multiple time stepping integration and extended to higher-order versions. These and other related problems will be the subject of a separate investigation.

ACKNOWLEDGMENT

Part of this work was supported by the Fonds zur Förderung der wissenschaftlichen Forschung under Project No. P12422-TPH.

[1] K. Chen and D.P. Landau, Phys. Rev. B **49**, 3266 (1994).
[2] A. Bunker, K. Chen, and D.P. Landau, Phys. Rev. B **54**, 9259 (1996).
[3] H.G. Evertz and D.P. Landau, Phys. Rev. B **54**, 12 302 (1996).
[4] B.V. Costa, J.E.R. Costa, and D.P. Landau, J. Appl. Phys. **81**, 5746 (1997).
[5] M. Krech, A. Bunker, and D.P. Landau, Comput. Phys. Commun. **111**, 1 (1998).
[6] D.P. Landau and M. Krech, J. Phys.: Condens. Matter **11**, R179 (1999).
[7] D.P. Landau, S.-H. Tsai, M. Krech, and A. Bunker, Int. J. Mod. Phys. C **10**, 1541 (1999).
[8] S.-H. Tsai, A. Bunker, and D.P. Landau, Phys. Rev. B **61**, 333 (2000).
[9] I.P. Omelyan, I.M. Mryglod, and R. Folk, Europhys. Lett. **52**, 603 (2000).
[10] E. Lomba, J.J. Weis, N.G. Almarza, F. Bresme, and G. Stell, Phys. Rev. E **49**, 5169 (1994).
[11] J.M. Tavares, M.M.T. Gama, P.I.C. Teixeira, J.J. Weis, and M.J.P. Nijmeijer, Phys. Rev. E **52**, 1915 (1995).
[12] I.M. Mryglod, M.V. Tokarchuk, and R. Folk, Physica A **220**, 325 (1995).
[13] M.J.P. Nijmeijer and J.J. Weis, Phys. Rev. Lett. **75**, 2887 (1995).
[14] M.J.P. Nijmeijer and J.J. Weis, Phys. Rev. E **53**, 591 (1996).
[15] I. Mryglod, R. Folk, S. Dubyk, and Yu. Rudavskii, Physica A **277**, 389 (2000).
[16] I.P. Omelyan, I.M. Mryglod, and R. Folk, Condens. Matter Phys. **3**, 497 (2000).
[17] I.P. Omelyan, I.M. Mryglod, and R. Folk, Phys. Rev. Lett. **86**, 898 (2001).
[18] M. Suzuki and K. Umeno, in *Computer Simulation Studies in Condensed Matter Physics VI*, edited by D.P. Landau, K.K. Mon, and H.B. Schüttler (Springer, Berlin, 1993).
[19] W.C. Swope, H.C. Andersen, P.H. Berens, and K.R. Wilson, J. Chem. Phys. **76**, 637 (1982).
[20] R.L. Burden and J.D. Faires, *Numerical Analysis*, 5th ed. (PWS, Boston, 1993).
[21] M.P. Allen and D.J. Tildesley, *Computer Simulation of Liquids* (Clarendon, Oxford, 1987).
[22] I.M. Mryglod, I.P. Omelyan, and R. Folk, Phys. Rev. Lett. **86**, 3156 (2001).
[23] D. Frenkel and B. Smit, *Understanding Molecular Simulation: from Algorithms to Applications* (Academic, New York, 1996).
[24] I.M. Mryglod, I.P. Omelyan, and M.V. Tokarchuk, Mol. Phys. **84**, 235 (1995).
[25] D. Greenspan, Comput. Math. Appl. **29**, 37 (1995).
[26] O. Gonzalez and J.C. Simo, Comput. Methods Appl. Mech. Eng. **134**, 197 (1996).